MDPO: Overcoming the Training-Inference Divide of Masked Diffusion Language Models

Haoyu He, Katrin Renz, Yong Cao, Andreas Geiger

University of Tübingen, Tübingen AI Center

{haoyu.he,katrin.renz,yong.cao,a.geiger}@uni-tuebingen.de

Abstract

Diffusion language models, as a promising alternative to traditional autoregressive (AR) models, enable faster generation and richer conditioning on bidirectional context. However, they suffer from a key discrepancy between training and inference: during inference, MDLMs progressively reveal the structure of the generated sequence by producing fewer and fewer masked tokens, whereas this structure is ignored in training as tokens are masked at random. Although this discrepancy between training and inference can lead to suboptimal performance, it has been largely overlooked by previous works, leaving closing this gap between the two stages an open problem. To address this, we frame the problem of learning effective denoising trajectories as a sequential decision-making problem and use the resulting framework to apply reinforcement learning. We propose a novel Masked Diffusion Policy Optimization (MDPO) to exploit the Markov property diffusion possesses and explicitly train the model under the same progressive refining schedule used at inference. MDPO matches the performance of the previous state-of-the-art (SOTA) method with 60× fewer gradient updates, while achieving average improvements of 9.6% on MATH500 and 54.2% on Countdown over SOTA when trained within the same number of weight updates. Additionally, we improve the remasking strategy of MDLMs as a plug-in inference replacement to overcome the limitation that the model cannot refine tokens flexibly. This simple yet effective training-free strategy, what we refer to as RCR, consistently improves performance and yields additional gains when combined with MDPO. Our findings establish great potential for investigating the discrepancy between pre-training and inference of MDLMs. Code: https://github.com/autonomousvision/mdpo. Project Page: https://cli212.github.io/MDPO/.

1 Introduction

Remarkable advances in language modeling have largely been driven by the autoregressive (AR) paradigm (Hochreiter & Schmidhuber, 1997; Vaswani et al., 2017), where tokens are generated in a causal fashion. An alternative line of work, Diffusion Language Models (DLMs) generates by iteratively denoising, enabling parallel prediction, bidirectional conditioning and faster generation speed. Recently, DLMs such as Mercury Coder (Khanna et al., 2025), Google Gemini Diffusion (Google DeepMind, 2025), and Seed Diffusion (Song et al., 2025) have emerged as promising alternatives that excel at external math and coding benchmarks. Built upon theoretical insights and practical optimizations in the discrete diffusion framework (Lou et al., 2024; Sahoo et al., 2024; Ou et al., 2025), Masked Diffusion Language Models (MDLMs) leads the current development of DLMs. Diffusion gradually adds noise to data in the forward process, and the model learns to reverse this corruption in the backward process. In the forward process of MDLMs, tokens are randomly chosen to either remain stationary or transition to a predefined absorbing state, such as a special masking token, motivated by the success of BERT (Devlin et al., 2019). Then in the backward process, the model learns to invert the noise by predicting *all* masked tokens conditioned on partially observed (unmasked) context. For generating a sequence of tokens, MDLMs alternates between predicting masked tokens and selectively remasking a fraction of the predictions based on heuristics and uncali-
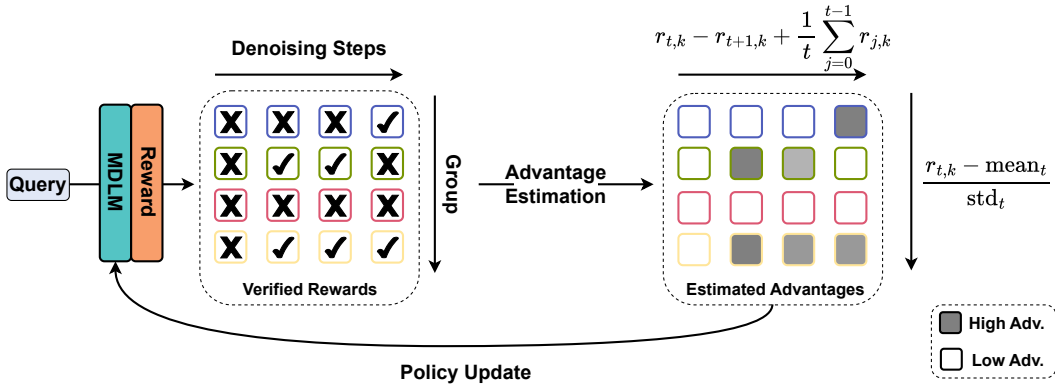
Figure 1: **MDPO** generates a group of answers given a query for RL rollouts. Then all completions at intermediate and final steps are verified with a reward model. Based on verified rewards, MDPO estimates the advantage of step t by considering rewards of the other steps in the current rollout and step t from other rollouts in the group. These estimated advantages are used for policy optimization.

brated token-wise scores.. Representative works as LLaDA-8B (Nie et al., 2025) and Dream-7B (Ye et al., 2025) demonstrate competitive performance to their similarly sized AR counterparts.

Despite promising empirical results, we identify two fundamental, largely overlooked problems of MDLMs that hinder effective denoising trajectories. (1) The *training–inference divide*: at inference time, MDLMs follow a model-dependent, confidence-guided unmasking schedule that progressively reveals structure of the generated sequence. By contrast, training masks tokens randomly at sampled diffusion steps, ignoring this progressive schedule. This mismatch prevents the model from learning effective denoising trajectories and often causes Answer Backslide: correct intermediate solutions that are 'refined' into wrong final outputs. (2) The common remasking approaches freeze tokens once predicted, making it impossible to revise early low-confidence predictions later. We address these problems with complementary methods in this work. MDPO casts denoising as a multi-step decision-making process, explicitly training the model under the same progressive, model-dependent unmasking schedule used at inference. By using reinforcement learning with intermediate rewards to optimize these trajectories, MDPO aligns training with actual inference dynamics, closing the training–inference divide. Running Confidence Remasking (RCR) is a training-free decoding strategy that tracks per-position confidence over time, enabling flexible remasking and revision of low-confidence tokens at any step. In summary, our contributions are three-fold:

- **Answer Backslide:** We observe a novel and previously unknown phenomenon in MDLMs: models occasionally produce correct answers at intermediate steps but 'refine' them into incorrect results. We refer to this phenomenon as Answer Backslide, which inspires us to supervise models not only on the final results but also intermediate denoising steps.

- **Masked Diffusion Policy Optimization (MDPO):** We propose MDPO to learn effective denoising trajectories without direct supervision. By exploiting the fact that MDLMs yield complete generations at every inference step, MDPO optimizes the model with policy gradients via intermediate-step rewards. Unlike prior RL fine-tuning on MDLMs, MDPO explicitly targets addressing the *training-inference divide* overlooked by previous works.

- **Running Confidence Remasking (RCR):** Instead of freezing tokens based on their single-step confidence, RCR allows flexible remasking by continuously tracking the running lowest confidence over denoising trajectories. Our experiments demonstrate consistently improved performance of using RCR on both LLaDA pre-trained as well as MDPO fine-tuned models.

Empirical results on challenging mathematical and reasoning benchmarks show that both MDPO and the training-free RCR substantially improve generation quality and sample efficiency. Our findings underscore the value of addressing the training-inference divide for masked diffusion language models and open new directions for research in this emerging paradigm.

2 RELATED WORK

2.1 DIFFUSION LANGUAGE MODELS

Diffusion probabilistic models (Sohl-Dickstein et al., 2015; Ho et al., 2020) have become the de facto standard for generative modeling in continuous domains, including images, videos, 3D shapes, and robotic trajectories. Building on early efforts in discrete diffusion (Austin et al., 2021; Hoogeboom et al., 2021), several works have adapted diffusion models for text generation. Diffusion-LM (Li et al., 2022) and Self-Conditioned Embedding Diffusion (Strudel et al., 2022) have pioneered embedding-based diffusion approaches, achieving comparable performance to AR methods. Liu et al. (2025) introduces a novel framework that separates the generation process into two models: a planner and a denoiser. Meanwhile, masked diffusion has been established as a special case of discrete diffusion processes (Austin et al., 2021; Sahoo et al., 2024; Ou et al., 2025), with recent research significantly scaling their capabilities. Notably, DiffuLLaMA (Gong et al., 2025) initializes masked diffusion language models using pretrained LLaMA weights. Block Diffusion (Arriola et al., 2025) models sequences in autoregressive blocks with intra-block diffusion, enabling variable-length generation and faster inference via KV caching. LLaDA (Nie et al., 2025) and Dream (Ye et al., 2025) scale MDLMs by pre-training from scratch to the billion-parameter regime, achieving performance comparable to similarly sized AR LLMs.

Beyond scaling, diffusion models have also shown promise in reasoning tasks. Ye et al. (2024) demonstrates that DLMs are effective in producing chain-of-thought reasoning and addressing complex reasoning tasks, even with smaller-scale models. These findings highlight diffusion models as a viable alternative to traditional AR methods. Kim et al. (2025); Wang et al. (2025) show that though MDLMs face inherently harder training challenges due to solving many computationally intractable infilling tasks, using adaptive decoding strategies dramatically overcomes these limitations. Our proposed Running Confidence Remasking builds upon these and shows that enabling the model to iteratively revise early-predicted 'noisy' tokens substantially enhances downstream performance.

2.2 TRAINING DIFFUSION MODELS WITH REINFORCEMENT LEARNING

Reinforcement learning has been primarily explored in training image diffusion models (Black et al., 2024; Fan et al., 2023) on non-differentiable downstream objectives such as human-perceived image quality or drug effectiveness. RL has emerged as a promising tool to optimize such sparse and task-specific reward signals (Yu et al., 2025; Shao et al., 2024; Luo et al., 2025b;a; Hu et al., 2025; Zeng et al., 2025). In language modeling, reinforcement learning has been extensively applied to AR LLMs, where post-training with reward-based fine-tuning significantly boosts reasoning capabilities (Guo et al., 2025; Luo et al., 2025b;a; Zeng et al., 2025; Hu et al., 2025). These RL algorithms are tailored for sequential token-by-token generation, a key property of AR models. However, MDLMs follow a fundamentally different paradigm: they are trained to predict complete text generations given randomly corrupted text, and iteratively refine the generations with fewer and fewer masked tokens at inference time. This prevents RL algorithms designed for AR models from being directly applied to DLMs. Zhao et al. (2025) made the first effort in this direction by adapting pretrained MDLMs to RL using Group Relative Policy Optimization (GRPO) (Shao et al., 2024), a policy optimization algorithm originally designed for AR models. In contrast, our work introduces MDPO, a policy optimization method designed for MDLMs to learn effective denoising trajectories by optimizing the iterative denoising process as a multi-step decision-making problem. To our knowledge, MDPO is the first RL method specifically designed to optimize the denoising trajectory of MDLMs.

3 METHODOLOGY

3.1 MASKED LANGUAGE DIFFUSION MODELS

We first provide the formulation of LLaDA (Nie et al., 2025), a pre-trained MDLM that serves as the foundation of our work. While specific architectural or methodological variations may exist among other MDLMs, the methods proposed in this paper are broadly applicable to the majority of existing MDLM frameworks. LLaDA defines a model distribution $p_\theta(x_0)$ of the clean data x_0 through a discrete diffusion process (Ou et al., 2025; Austin et al., 2021). The forward process gradually masks tokens until the sequence is fully masked. The reverse process recovers $p_\theta(x_0)$ by iteratively predicting masked tokens.

Training: The training objective optimizes a mask predictor $p_\theta\left(x_0 \mid \bar{x}_\tau\right)$ that takes partially masked data $\bar{x}_\tau$[1] as input and predicts all masked tokens simultaneously using a cross-entropy loss:

$$\mathcal{L}(\theta) \triangleq -\mathbb{E}_{x_0,\tau}\left[\frac{1}{\tau}\sum_{i=1}^{L}\mathbb{1}[\bar{x}_\tau^i = \mathcal{M}]\,\log p_\theta\left(x_0^i \mid \bar{x}_\tau\right)\right] \qquad \bar{x}_\tau \triangleq \tilde{\gamma}(x_0, \tau) \qquad (1)$$

Here, the expectation is computed over the unmasked ground truth sequences $\{x_0\}$ in the dataset and a randomly drawn masking ratio $\tau \sim U(0,1)$. $\tilde{\gamma}(x_0, \tau)$ is a masking function that sets each token of x_0 to the mask token $\mathcal{M}$ independently with probability τ. L is the sequence length and superscript i for both x and $\bar{x}$ denotes the i'th element in the sequence. The cross-entropy loss is only computed on the masked tokens as indicated by the function $\mathbb{1}[\cdot]$. In practice, $p_\theta\left(x_0 \mid \bar{x}_\tau\right)$ often depends on an additional input prompt which we drop here for notational clarity.

Inference: Inference of LLaDA involves iterative refinement from a fully masked input, progressively reducing the number of masked tokens at each step t. This is necessary, as the initial noise contains no structure and the mapping from noise to the generated sequence is highly non-linear and multimodal (Xiao et al., 2022; Song et al., 2021). Hence, multiple iterations (each conditioning on the structure generated so far) are required to achieve coherent, contextually and syntactically consistent outputs (Nie et al., 2025; Feng et al., 2025). Given T denoising steps, the inference starts from a fully masked sequence $\bar{x}_T = (\mathcal{M}, \ldots, \mathcal{M})$ and alternates the following two steps:

1. Given a masked sequence $\bar{x}_t$, draw all masked tokens by sampling from $x_{t-1} \sim p_\theta(\cdot \mid \bar{x}_t)$ to produce a *fully unmasked* sequence x_{t-1}.

2. Remask x_{t-1} using a confidence-based remasking function γ yielding a *partially masked* sequence $\bar{x}_{t-1}$. More specifically, with decreasing t, LLaDA remasks a decreasing number of tokens based on the current model's confidence score $1 - p_\theta(x_{t-1}^i \mid \bar{x}_t)$

LLaDA continues this process until time step $t = 0$. The confidence-based remasking strategy (2) reveals more and more structure for $p_\theta(x_{t-1}|\bar{x}_t)$ to condition on over time. The number of denoising steps T is a hyperparameter providing a trade-off between efficiency and quality (Nie et al., 2025). We refer the reader to Section 3.4 for details about the implementation of the remasking function γ.

3.2 THE TRAINING-INFERENCE DIVIDE

The above formulation of LLaDA reveals an important discrepancy between training and inference: specifically, during training, the model is optimized to predict all masked tokens at randomly chosen masking ratios τ. In contrast, inference involves multiple iterative denoising steps informed by the model's confidence score, forming a trajectory with fewer and fewer masked tokens to be predicted, and more and more structure being revealed. However, this structure is ignored during training, where at each iteration tokens are masked at random. This leads to a *training-inference divide* which limits the performance of the model as it is unable to learn effective diffusion trajectories.

Task	Acc.
MATH-500	18.2
w/ inter. ans	+9.8
Countdown	38.7
w/ inter. ans	+6.2

Table 1: Accuracy of LLaDA on two verifiable tasks and the ratio of at least one out of 256 intermediate steps is correct (w/ inter.ans).

We observe symptoms of this behavior by inspecting denoising trajectories of pre-trained MDLMs. Table 1 shows the accuracy of LLaDA on two reasoning tasks and the additional accuracy if we count intermediate-step correct answers that are 'refined' into wrong final answers. We refer to this phenomenon as Answer Backslide and do detailed studies in Section 4.3.

A simple solution to address this discrepancy would be to fine-tune the model with ground-truth trajectories. However, such trajectories are inherently unavailable, as human-generated data does not capture iterative denoising paths. In this paper, we hence investigate the following question:

> How can we learn effective discrete diffusion trajectories without direct supervision?

A key advantage of masked language diffusion models over traditional auto-regressive models is that they yield *complete* text generations at *every* inference step. This allows for evaluating the quality of

---

[1]We use the bar notation (e.g. $\bar{x}$) to denote masked and x for unmasked sequences throughout the paper.

intermediate generations using an appropriately chosen reward model. In this paper, we propose to exploit this property to effectively fine-tune diffusion policies using deep reinforcement learning. To focus our analysis, we investigate reasoning tasks with verifiable answers, such as math problems. However, we remark that other problems without verifiable answers can also be addressed within our framework using modern validation concepts such as LLM-as-a-judge (Li et al., 2024).

3.3 MASKED DIFFUSION POLICY OPTIMIZATION (MDPO)

While reinforcement learning (RL) has originally been applied to address sequential decision-making tasks, it emerges as a promising alternative for optimizing deep neural networks to maximize non-differentiable objectives (Mnih et al., 2013; François-Lavet et al., 2018; Ouyang et al., 2022). Recognizing inference in MDLMs as a sequential decision-making problem, we propose to explicitly train the mask prediction network as an RL policy (Jaeger & Geiger, 2024). Policy gradient methods train a policy network $\pi(a \mid s)$ that predicts a probability distribution over actions using non-differentiable rewards by maximizing the expected return:

$$\mathcal{J}(\pi) = \mathbb{E}_{(s,a)} \left[\pi(a \mid s) \, r(s,a) \right] \tag{2}$$

where the expectation is computed over state-action pairs (s, a) collected on-policy and $r(s, a)$ is a reward function. Linking MDLMs to policy gradient methods, each denoising step corresponds to an action that predicts all masked tokens in a (partially) masked sequence $\bar{x}_t$, with reward $r(x_{t-1})$ via an evaluation model $r(\cdot)$.

The expected return of our Masked Diffusion Policy Optimization (MDPO) model is:

$$\mathcal{J}(\theta) \triangleq \mathbb{E}_{\{x_T,..,x_0\} \sim p_\theta} \left[\sum_{t=1}^{T} \sum_{i=1}^{L} \mathbb{1}[\bar{x}_t^i = \mathcal{M}] \, \log p_\theta(x_{t-1}^i \mid \bar{x}_t) \, r(x_{t-1}) \right] \qquad \bar{x}_t \triangleq \gamma(x_t, t) \tag{3}$$

where the expectation is computed over denoising trajectories $\{x_T, \ldots, x_0\}$ generated by the current denoising policy p_θ. We use the same masking function $\gamma(x_t, t)$ as used during inference, which takes an unmasked sequence x_t as input and converts it into a (partially) masked sequence $\bar{x}_t$ depending on the current time step t. The smaller the timestep, the fewer tokens are masked (see Section 3.4 for details). The indicator function aggregates the return only at locations where the input is masked. The denoising policy models the probability distribution of the denoised token x_{t-1}^i at location i given the masked input at the previous time step $\bar{x}_t$. Again, we drop the prompt here for notational clarity.

As the gradients must be computed from data generated by the current policy p_θ, the policy gradient estimator defined in Eq. (3) only allows a single optimization step for each round of data collection. To enable multiple steps of optimization, we use importance sampling (Kakade & Langford, 2002; Black et al., 2024) and the clipped surrogate objective from Proximal Policy Optimization (PPO) (Schulman et al., 2017). Moreover, inspired by the effectiveness of group-relative advantage estimation (Shao et al., 2024), we sample a group of G trajectories $\{x_{t,1}, \ldots, x_{t,G}\}$ at each step t from the old policy $p_{\theta_{\text{old}}}$ to update the current policy p_θ, see Fig. 1 for demonstration. Our final objective is given by:

$$\mathcal{J}(\theta) \triangleq \mathbb{E}_{\{x_{T,k}, \ldots, x_{0,k}\}_{k=1}^{G} \sim p_{\theta_{\text{old}}}} \left[\frac{1}{G} \sum_{k=1}^{G} \sum_{t=1}^{T} \sum_{i=1}^{L} \mathbb{1}[\bar{x}_{t,k}^i = \mathcal{M}] \left(Z_{t,k}^i - \beta \mathbb{D}_{KL} \left[p_\theta || p_{\text{ref}} \right] \right) \right] \tag{4}$$

Here, p_{ref} is the reference model which is usually the initial model before training, $\mathbb{D}_{KL} \left[p_\theta || p_{\text{ref}} \right]$ is the KL divergence between the trained model p_θ and the reference model. $Z_{t,k}^i$ is the clipped and weighted advantage (Schulman et al., 2017)

$$Z_{t,k}^i = \min \left[\frac{p_\theta(x_{t-1,k}^i \mid \bar{x}_{t,k})}{p_{\theta_{\text{old}}}(x_{t-1,k}^i \mid \bar{x}_{t,k})} A_{t-1,k}, \text{clip} \left(\frac{p_\theta(x_{t-1,k}^i \mid \bar{x}_{t,k})}{p_{\theta_{\text{old}}}(x_{t-1,k}^i \mid \bar{x}_{t,k})}, 1 - \epsilon, 1 + \epsilon \right) A_{t-1,k} \right] \tag{5}$$

where ϵ and β are hyper-parameters. $A_{t,k}$ is the advantage of x_t in the k'th group calculated based on relative rewards inside each group:

$$A_{t,k} = \frac{s_{t,k} - \text{mean}(\{s_{t,1}, s_{t,2}, \cdots, s_{t,G}\})}{\text{std}(\{s_{t,1}, s_{t,2}, \cdots, s_{t,G}\})} \qquad s_{t,k} = r(x_{t,k}) - r(x_{t+1,k}) + \frac{1}{t} \sum_{j=0}^{t-1} r(x_{j,k}) \tag{6}$$

In GRPO, group-relative advantage estimation optimizes the memory usage of training LLMs with RL by dropping the jointly trained value model that is originally used to predict the advantages.

Beyond this, another intuitive reason to use group-relative advantage estimation in the diffusion setting is to incentivize better generation with fewer denoising steps. Specifically, by comparing to a group of trajectories, steps reaching the final reward more rapidly are assigned higher advantages. In addition, Eq. (6) encourages each denoising step to (i) make an immediate improvement over the previous, noisier prediction and (ii) steer the trajectory toward cleaner states that score well overall.

3.4 REMASKING

As introduced in Section 3.1, inference in LLaDA alternates between predicting all masked tokens in $\bar{x}_t$ and selectively re-masking a fraction of the prediction x_{t-1} via $\bar{x}_{t-1} = \gamma(x_{t-1}, t)$ for iterative refinement. We first discuss random and confidence-based re-masking as introduced in LLaDA. Next, we propose a simple yet effective improvement to address a key limitation of confidence-based re-masking, which consistently leads to better performance for both LLaDA pre-trained as well as MDPO fine-tuned models. Formally, the remasking function γ assigns the mask symbol $\mathcal{M}$ to the tokens with the n_t'th highest masking scores:

$$\gamma(x_t, t) = \begin{cases} \mathcal{M} & \text{if } m_t^i \geq (n_t\text{'th highest value of } m_t) \\ x_t^i & \text{otherwise} \end{cases} \tag{7}$$

where $n_t = \lfloor \phi(t, T)L \rfloor$ determines the number of tokens to be masked depending on the time step t and a scheduling function ϕ. n_t decreases as t increases (more tokens are masked for larger t). m_t^i is a generic definition of the masking score of token i at step t and remasking strategies vary in how they compute m_t^i. LLaDA applies a linear function for ϕ so that an equal amount of $\lfloor \frac{L}{T} \rfloor$ tokens are *not* remasked every step, i.e., $n_t = \lfloor \frac{T-t}{T}L \rfloor$. We investigate various schedules in Appendix A.2.

Random Remasking (RR): A simple baseline to construct masking scores is random sampling:

$$m_{t-1}^i \sim \mathcal{U}(0, 1) \qquad \forall_{t,i} : \bar{x}_t^i = \mathcal{M} \tag{8}$$

While random sampling is consistent with the LLaDA training objective (Section 3.1), which masks tokens randomly, this strategy performs poorly in practice (Nie et al., 2025) as it doesn't exploit the structure of natural diffusion trajectories.

Low-Confidence Remasking (LCR): Inspired by the annealing tricks of sampling in AR LLMs (Holtzman et al., 2020), LLaDA proposes to utilize the model's prediction confidence as the masking scores:

$$m_{t-1}^i = 1 - p_\theta(x_{t-1}^i \mid \bar{x}_t) \qquad \forall_{t,i} : \bar{x}_t^i = \mathcal{M} \tag{9}$$

Empirical evaluations demonstrate that this model-derived low-confidence remasking significantly outperforms random masking in downstream tasks.

Running Confidence Remasking (RCR): An important observation is that both remasking strategies above (used in LLaDA) assign masking scores only to predicted tokens in x_t that were masked before. The unmasked tokens remain fixed until the end of the denoising process. In other words, if x_t^i is not remasked by $\gamma(x_t, t)$, it will be unmasked (frozen) in the following steps $x_{<t}^i$. We consider this a crucial limitation, as the predicted tokens, particularly in the early steps, tend to be highly noisy due to the limited structure revealed at that stage. Freezing these noisy tokens until the end of the denoising process makes it more difficult to produce high-quality generation in practice.

To address this, we propose Running Confidence Remasking (RCR). Instead of deciding based solely on the confidence at the current step, we track for each position i the highest confidence it has achieved so far for predicting masked tokens during the denoising process. At each step, we identify the n_t positions whose running maximum confidence is the lowest and remask tokens at these positions. Formally, for token i at step t, let t' index any earlier step in the denoising process ($t \leq t' \leq T$), the masking score is defined as:

$$m_{t-1}^i = 1 - \max_{t' \geq t} \left(p_\theta(x_{t'-1}^i \mid \bar{x}_{t'}) \right) \qquad \forall_{t,i} : \bar{x}_t^i = \mathcal{M} \tag{10}$$

Tokens at positions with higher running maximum confidence get lower masking scores (less likely to be remasked), while those that have never reached high confidence remain candidates for remasking.

Empirically, with more structure being revealed along with denoising, earlier steps often yield low-confidence predictions, whereas later steps tend to converge to higher confidence. Under the LCR
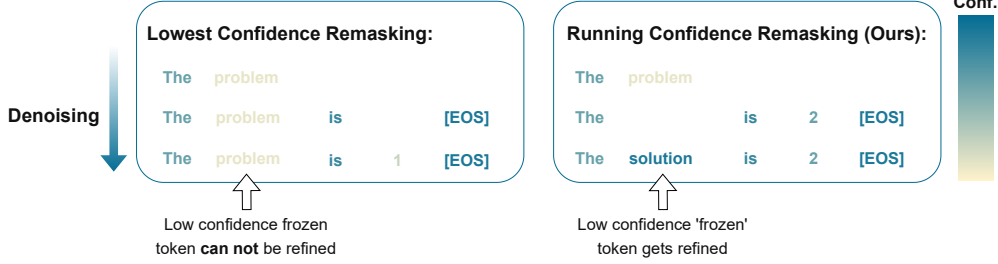
Figure 2: Comparison between Lowest Confidence Remasking (LCR) and our proposed Running Confidence Remasking (RCR) during iterative denoising. For each step, we show tokens that are *not* remasked. LCR freezes low-confidence tokens once unmasked, preventing further refinement, which potentially accumulates early-stage noise. For example, the token 'problem' predicted and frozen by LCR at step 1 is wrong but maintained until the end of the denoising, which leads to the final wrong answer. Whereas RCR tracks the running maximum confidence for each position, allowing persistently low-confidence tokens to be refined in later steps, leading to higher-quality completions.

strategy, early tokens are retained despite their relatively low confidence if they happen to fall within the top-n_t set at that step and can not be refined in future steps. In contrast, as Fig. 2 shows, RCR allows such tokens to be remasked in later steps if tokens at other positions surpass them in running confidence, enabling the model to revise uncertain predictions before producing the final output.

4 EXPERIMENTS

Our experiments are designed to address three core questions:

1. How do MDPO and RCR improve generation performance and sampling efficiency, and are their effects complementary?
2. Recognizing Answer Backslide as a manifestation of the training–inference divide, how can we leverage it to close this gap?
3. What is the impact of different sampling settings during MDPO training?

4.1 EXPERIMENTAL SETUP

Inference: The performance of MDLMs depends on several inference-time hyperparameter choices. A key distinction lies in whether denoising is performed over the full sequence at once or in blocks. Previous works apply a semi-autoregressive strategy where the sequence is divided into several blocks and generated from left to right. Within each block, tokens are denoised in parallel. We refer to this setting as *semi-AR*, and contrast it with the setting of denoising all tokens in the entire sequence simultaneously (*pure-Diff*). In semi-AR, the same remasking strategies used in pure-Diff apply, but each block denoises fewer tokens with fewer steps. To generate a sequence of length L with block size B in T steps, each block is allocated approximately $\lfloor \frac{T \cdot B}{L} \rfloor$ steps. As shown in Fig. 6, performance varies significantly depending on the choice of B and T. For controlled comparisons, we adopt two standard configurations throughout our experiments: pure-Diff ($B = L$) and semi-AR ($B = 128$). Extensive analysis on choices of block size is in Appendix A.3. Though empirically the pure-Diff setting usually underperforms semi-AR, we keep it as an interesting setting in our main evaluation because of the potential speed advantage that pure-Diff possesses at generating long responses.

Data: We investigate reasoning tasks with answers that can be verified by static reward functions: (1) MATHEMATICAL REASONING where the model generates solutions to mathematical problems and we verify if the ground truth answers are in the solutions with a robust mathematical expression evaluation system (Kydlíček & Gandenberger, 2025). Note that different math verifiers can lead to changes in evaluation results and we control the experiments by consistently use the same verifier. (2) PLANNING with Countdown (Pan et al., 2025), an easy-to-verify combinatorial arithmetic game in which the model tries to reach target numbers using basic arithmetic operations on a given set (3 or 4) of numbers. Evaluation is on MATH-500 (Lightman et al., 2024), a curated dataset of 500 problems

Table 2: **Model performance on Mathematics and Countdown: Best** and second-best methods in each setting are shaded. For each task we report results on semi-AR (Block Size = 128) and pure-Diff (Block Size = 512) given the generation length of 512. We also compare the performance across multiple choices of denoising steps.

	MATH500						Countdown					
Block Size	**128**			**512**			**128**			**512**		
Model / Steps	**64**	**128**	**256**	**64**	**128**	**256**	**64**	**128**	**256**	**64**	**128**	**256**
LLaDA-8B-Instruct	20.0	36.2	39.4	20.0	22.6	18.2	5.5	18.8	20.7	14.8	33.6	38.7
+ SFT (Nie et al., 2025)	18.0	33.8	41.8	22.2	24.6	25.4	12.3	20.7	28.6	35.5	43.1	49.6
+ diffu-GRPO (Zhao et al., 2025)	23.8	34.4	40.2	21.2	26.2	20.6	18.2	35.9	40.1	49.4	55.0	58.9
+ RCR (training-free)	25.4	37.6	40.8	22.6	22.6	19.2	9.4	15.2	26.6	32.8	43.8	45.7
+ MDPO	26.2	38.6	42.8	23.4	25.2	26.2	64.8	70.7	70.7	68.4	68.8	71.1
+ MDPO + RCR	30.4	38.4	44.2	24.8	24.0	26.4	69.9	70.7	73.4	67.2	69.5	57.4

from the MATH dataset (Hendrycks et al., 2021); and the Countdown test set by Zhao et al. (2025), specifically. For training on the mathematical reasoning task, we utilize (part of) the math data from Huggingface OpenR1 (Hugging Face, 2025) that consists of 93.7k competition-level math problems from NuminaMath 1.5 (LI et al., 2024). For Countdown, we directly use the respective training split released by Pan et al. (2025).

Model and Training: We compare our methods to two baseline methods: diffu-GRPO (Zhao et al., 2025), which is the first integration of policy gradient methods trained on MDLMs, and LLaDA with supervised finetuning (SFT). We (re)train both the baseline methods and MDPO initialized with LLaDA-8B-Instruct (Nie et al., 2025) under the same settings. Training of all methods is conducted under a fixed compute budget using 8 NVIDIA H100 GPUs with 100 weight update steps. We use a batch size of 128 and apply gradient accumulation when memory constraints occur. For both diffu-GRPO and our proposed MDPO, the group size for group-relative advantage estimation is 8, and the number of denoising steps for sampling rollouts is 128. One special setting that will be discussed in detail in Section 4.3 is that we train MDPO with *only* Answer Backslide samples, which shows better data efficiency.

4.2 Improvements in Generation Performance and Sample Efficiency

We first show the results (see Table 2) of our proposed Masked Diffusion Policy Optimization (MDPO) and training-free Running Confidence Remasking (RCR) compared to the baselines on MATH-500 and Countdown. Across all configurations, both MDPO and RCR individually improve substantially upon the LLaDA initialization, with RCR often achieving performance comparable to MDPO despite requiring no additional training. We remark that RCR, as a training-free method, even outperforms the training baselines in most of the settings for the MATH task. Notably, combining MDPO with RCR consistently yields further gains over either method alone, achieving the best or second-best performance in nearly all settings, which demonstrates that MDPO and RCR are complementary. We further observe that the relative performance gains are more pronounced in settings with fewer inference steps, indicating improved *sampling efficiency*.

Findings from Countdown: Furthermore, in Countdown, we observe a surprising behavioral shift: the model trained with MDPO transitions from generating explicit step-by-step reasoning to producing direct answers in a few (<10) steps. This echoes the advantages of diffusion models for latent reasoning discussed by previous work (Zhu et al., 2025). Another interesting observation is that pure-Diff (of LLaDA) substantially outperforms semi-AR on the Countdown task, which is rare on our math task and other tasks evaluated by the LLaDA paper. We hypothesize that this is due to the short expected reasoning traces for Countdown, where semi-AR uses fewer *effective* blocks as well as fewer *effective* denoising steps, limiting its ability to refine predictions. After MDPO training, as the model tends to directly produce answers without explicit reasoning, the performance
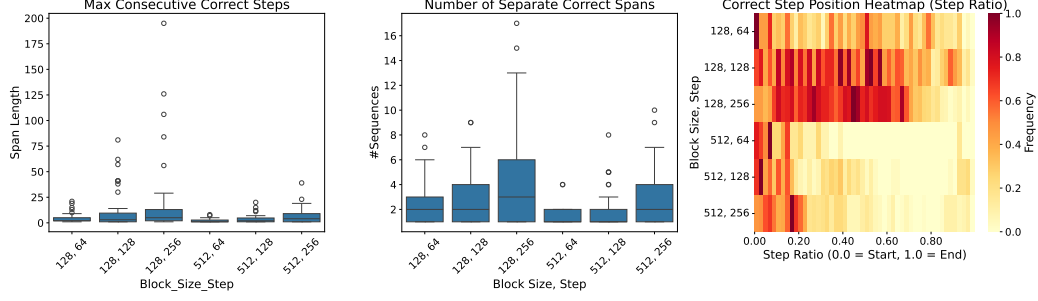
Figure 3: **Analysis of samples where Answer Backslide occur.** (Left) Maximum length of consecutive correct steps (span) in the denoising trajectory. (Middle) Number of separate correct spans in a trajectory. (Right) Heatmap of the relative position of correct steps across the denoising process.
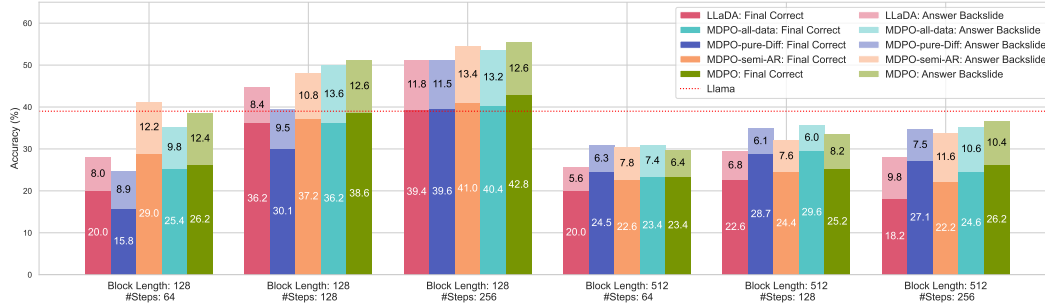

Figure 4: **Comparison of MDPO variants.** We report final accuracy and proportion of Answer Backslide cases for all models. MDPO-all-data is trained on all data samples whereas MDPO is trained on *only* Answer Backslide data, both with rollouts sampled from a mixture of semi-AR and pure-Diff. MDPO-pure-Diff and MDPO-semi-AR represent models that are trained on rollouts sampled from *only* pure-Diff, and semi-AR, respectively.

between pure-Diff and semi-AR gets closer. This observation highlights the flexibility of pure-Diff, particularly for tasks that do not require extended reasoning chains.

4.3 ANSWER BACKSLIDE IS AN EFFECTIVE DATA FILTER

We analyse the Answer Backslide phenomenon in more detail in Fig. 3 which reveals two key insights. First, the left and middle subfigures show that correct spans are typically short and fragmented, with trajectories often containing multiple separate correct spans instead of steadily accumulating correct steps. Such fragmentation increases the likelihood of losing correct tokens before reaching the final step. Second, the heatmap shows that correct answers often appear surprisingly very early but tend to decay over subsequent steps instead of steadily accumulating.

These findings not only underline the necessity to address the training-inference divide for MDLMs, but also reveal that Answer Backslide provides highly informative signals of intermediate steps for improving MDLMs. Inspired by this, we train MDPO with only Answer Backslide samples instead of all data so that MDPO can learn from these intermediate signals more efficiently. Specifically, we first use the initialized model to run inference on the whole dataset to identify Answer Backslide samples and then train only on this subset, which constitutes roughly 10% of the original data. The comparison between MDPO-all-data and MDPO in Fig. 4 shows that the model trained with only Answer Backslide excels in most settings, highlighting the effectiveness of Answer Backslide as a data filter for MDPO.

4.4 IMPACT OF SAMPLING SETTINGS ON MDPO

The heatmap in Fig. 3 shows that semi-AR tends to distribute correctness more evenly but with greater fragmentation, while pure-Diff produces an early burst of correctness that decays sharply and rarely recovers. This raises a question of how different sampling settings during the rollout collection of RL affect the final performance. To investigate this, we compare MDPO variants trained on (i)

pure-Diff rollouts only, (ii) semi-AR rollouts only, and (iii) an even mixture of both. Fig. 4 shows that training on a single mode yields the largest improvement in that mode's evaluation setting, but often at the cost of performance in the other mode. The mixture strategy used in our main MDPO setting achieves a more balanced performance, matching or exceeding the best single-mode results in several configurations. This suggests that mixed sampling allows the policy to learn denoising behaviors that generalize across all inference strategies.

5 CONCLUSION

This paper tackles the training–inference divide in Masked Diffusion Language Models (MDLMs) by proposing Masked Diffusion Policy Optimization (MDPO) and Running Confidence Remasking (RCR). MDPO uses reinforcement learning to optimize denoising trajectories with intermediate rewards, while RCR flexibly revisits earlier noisy predictions to reduce error propagation. One limitation of our work is that only verifiable tasks with static reward functions are investigated. We leave the application of MDPO to general tasks using modern validation concepts such as LLM-as-a-judge for intermediate rewards as future work.

REFERENCES

Marianne Arriola, Subham Sekhar Sahoo, Aaron Gokaslan, Zhihan Yang, Zhixuan Qi, Jiaqi Han, Justin T Chiu, and Volodymyr Kuleshov. Block diffusion: Interpolating between autoregressive and diffusion language models. 2025. 3

Jacob Austin, Daniel D. Johnson, Jonathan Ho, Daniel Tarlow, and Rianne van den Berg. Structured denoising diffusion models in discrete state-spaces. 2021. 3

Kevin Black, Michael Janner, Yilun Du, Ilya Kostrikov, and Sergey Levine. Training diffusion models with reinforcement learning. 2024. 3, 5

Huiwen Chang, Han Zhang, Lu Jiang, Ce Liu, and William T. Freeman. Maskgit: Masked generative image transformer. pp. 11305–11315, 2022. 14

Jacob Devlin, Ming-Wei Chang, Kenton Lee, and Kristina Toutanova. BERT: pre-training of deep bidirectional transformers for language understanding. 2019. 1

Ying Fan, Olivia Watkins, Yuqing Du, Hao Liu, Moonkyung Ryu, Craig Boutilier, Pieter Abbeel, Mohammad Ghavamzadeh, Kangwook Lee, and Kimin Lee. Reinforcement learning for fine-tuning text-to-image diffusion models. 2023. 3

Guhao Feng, Yihan Geng, Jian Guan, Wei Wu, Liwei Wang, and Di He. Theoretical benefit and limitation of diffusion language model. 2025. 4

Vincent François-Lavet, Peter Henderson, Riashat Islam, Marc G. Bellemare, and Joelle Pineau. An introduction to deep reinforcement learning. *Found. Trends Mach. Learn.*, 11(3-4):219–354, 2018. 5

Shansan Gong, Shivam Agarwal, Yizhe Zhang, Jiacheng Ye, Lin Zheng, Mukai Li, Chenxin An, Peilin Zhao, Wei Bi, Jiawei Han, Hao Peng, and Lingpeng Kong. Scaling diffusion language models via adaptation from autoregressive models. 2025. 3

Google DeepMind. Gemini diffusion: our state-of-the-art experimental text diffusion model, 2025. URL https://deepmind.google/models/gemini-diffusion/. 1

Daya Guo, Dejian Yang, Haowei Zhang, Junxiao Song, Ruoyu Zhang, Runxin Xu, Qihao Zhu, Shirong Ma, Peiyi Wang, Xiao Bi, et al. Deepseek-r1: Incentivizing reasoning capability in llms via reinforcement learning. 2025. 3

Dan Hendrycks, Collin Burns, Saurav Kadavath, Akul Arora, Steven Basart, Eric Tang, Dawn Song, and Jacob Steinhardt. Measuring mathematical problem solving with the MATH dataset. 2021. 8

Jonathan Ho, Ajay Jain, and Pieter Abbeel. Denoising diffusion probabilistic models. 2020. 3

Sepp Hochreiter and Jürgen Schmidhuber. Long short-term memory. *Neural Computation*, pp. 1735–1780, 1997. 1

Ari Holtzman, Jan Buys, Li Du, Maxwell Forbes, and Yejin Choi. The curious case of neural text degeneration. 2020. 6

Emiel Hoogeboom, Didrik Nielsen, Priyank Jaini, Patrick Forré, and Max Welling. Argmax flows and multinomial diffusion: Learning categorical distributions. 2021. 3

Jingcheng Hu, Yinmin Zhang, Qi Han, Daxin Jiang, Xiangyu Zhang, and Heung-Yeung Shum. Open-reasoner-zero: An open source approach to scaling up reinforcement learning on the base model. 2025. 3

Hugging Face. Open r1: A fully open reproduction of deepseek-r1, January 2025. URL https://github.com/huggingface/open-r1. 8

Bernhard Jaeger and Andreas Geiger. An invitation to deep reinforcement learning. *Found. Trends Optim.*, 7(1):1–80, 2024. 5

Sham Kakade and John Langford. Approximately optimal approximate reinforcement learning. pp. 267–274, 2002. 5

Samar Khanna, Siddhant Kharbanda, Shufan Li, Harshit Varma, Eric Wang, Sawyer Birnbaum, Ziyang Luo, Yanis Miraoui, Akash Palrecha, Stefano Ermon, Aditya Grover, and Volodymyr Kuleshov. Mercury: Ultra-fast language models based on diffusion. 2025. 1

Jaeyeon Kim, Kulin Shah, Vasilis Kontonis, Sham M. Kakade, and Sitan Chen. Train for the worst, plan for the best: Understanding token ordering in masked diffusions. 2025. 3

Hynek Kydlíček and Greg Gandenberger. Math-verify: A robust mathematical expression evaluation system. https://github.com/huggingface/Math-Verify, 2025. Version 0.8.0, released July 2, 2025. 7

Haitao Li, Qian Dong, Junjie Chen, Huixue Su, Yujia Zhou, Qingyao Ai, Ziyi Ye, and Yiqun Liu. Llms-as-judges: A comprehensive survey on llm-based evaluation methods. abs/2412.05579, 2024. 5

Jia LI, Edward Beeching, Lewis Tunstall, Ben Lipkin, Roman Soletskyi, Shengyi Costa Huang, Kashif Rasul, Longhui Yu, Albert Jiang, Ziju Shen, Zihan Qin, Bin Dong, Li Zhou, Yann Fleureau, Guillaume Lample, and Stanislas Polu. Numinamath. [https://huggingface.co/AI-MO/NuminaMath-1.5](https://github.com/project-numina/aimo-progress-prize/blob/main/report/numina_dataset.pdf), 2024. 8

Xiang Lisa Li, John Thickstun, Ishaan Gulrajani, Percy Liang, and Tatsunori B. Hashimoto. Diffusion-lm improves controllable text generation. 2022. 3

Hunter Lightman, Vineet Kosaraju, Yuri Burda, Harrison Edwards, Bowen Baker, Teddy Lee, Jan Leike, John Schulman, Ilya Sutskever, and Karl Cobbe. Let's verify step by step. 2024. 7

Sulin Liu, Juno Nam, Andrew Campbell, Hannes Stärk, Yilun Xu, Tommi S. Jaakkola, and Rafael Gómez-Bombarelli. Think while you generate: Discrete diffusion with planned denoising. 2025. 3

Aaron Lou, Chenlin Meng, and Stefano Ermon. Discrete diffusion modeling by estimating the ratios of the data distribution. 2024. 1

Michael Luo, Roy Huang Sijun Tan, Xiaoxiang Shi, Rachel Xin, Colin Cai, Ameen Patel, Alpay Ariyak, Qingyang Wu, Ce Zhang, Li Erran Li, Raluca Ada Popa, and Ion Stoica. Deepcoder: A fully open-source 14b coder at o3-mini level, 2025a. Notion Blog. 3

Michael Luo, Sijun Tan, Justin Wong, Xiaoxiang Shi, William Y. Tang, Manan Roongta, Colin Cai, Jeffrey Luo, Li Erran Li, Raluca Ada Popa, and Ion Stoica. Deepscaler: Surpassing o1-preview with a 1.5b model by scaling rl, 2025b. Notion Blog. 3

Volodymyr Mnih, Koray Kavukcuoglu, David Silver, Alex Graves, Ioannis Antonoglou, Daan Wierstra, and Martin A. Riedmiller. Playing atari with deep reinforcement learning. 2013. 5

Shen Nie, Fengqi Zhu, Zebin You, Xiaolu Zhang, Jingyang Ou, Jun Hu, Jun Zhou, Yankai Lin, Ji-Rong Wen, and Chongxuan Li. Large language diffusion models. 2502.09992, 2025. 2, 3, 4, 6, 8, 14

Jingyang Ou, Shen Nie, Kaiwen Xue, Fengqi Zhu, Jiacheng Sun, Zhenguo Li, and Chongxuan Li. Your absorbing discrete diffusion secretly models the conditional distributions of clean data. 2025. 1, 3

Long Ouyang, Jeffrey Wu, Xu Jiang, Diogo Almeida, Carroll Wainwright, Pamela Mishkin, Chong Zhang, Sandhini Agarwal, Katarina Slama, Alex Gray, John Schulman, Jacob Hilton, Fraser Kelton, Luke Miller, Maddie Simens, Amanda Askell, Peter Welinder, Paul Christiano, Jan Leike, and Ryan Lowe. Training language models to follow instructions with human feedback. 2022. 5

Jiayi Pan, Junjie Zhang, Xingyao Wang, Lifan Yuan, Hao Peng, and Alane Suhr. Tinyzero. https://github.com/Jiayi-Pan/TinyZero, 2025. Accessed: 2025-01-24. 7, 8

Subham S. Sahoo, Marianne Arriola, Yair Schiff, Aaron Gokaslan, Edgar Marroquin, Justin T. Chiu, Alexander Rush, and Volodymyr Kuleshov. Simple and effective masked diffusion language models. 2024. 1, 3

John Schulman, Filip Wolski, Prafulla Dhariwal, Alec Radford, and Oleg Klimov. Proximal policy optimization algorithms. 2017. 5

Zhihong Shao, Peiyi Wang, Qihao Zhu, Runxin Xu, Junxiao Song, Xiao Bi, Haowei Zhang, Mingchuan Zhang, YK Li, Y Wu, et al. Deepseekmath: Pushing the limits of mathematical reasoning in open language models. 2024. 3, 5

Jascha Sohl-Dickstein, Eric A. Weiss, Niru Maheswaranathan, and Surya Ganguli. Deep unsupervised learning using nonequilibrium thermodynamics. 2015. 3

Jiaming Song, Chenlin Meng, and Stefano Ermon. Denoising diffusion implicit models. 2021. 4

Yuxuan Song, Zheng Zhang, Cheng Luo, Pengyang Gao, Fan Xia, Hao Luo, Zheng Li, Yuehang Yang, Hongli Yu, Xingwei Qu, Yuwei Fu, Jing Su, Ge Zhang, Wenhao Huang, Mingxuan Wang, Lin Yan, Xiaoying Jia, Jingjing Liu, Wei-Ying Ma, Ya-Qin Zhang, Yonghui Wu, and Hao Zhou. Seed diffusion: A large-scale diffusion language model with high-speed inference. 2025. 1

Robin Strudel, Corentin Tallec, Florent Altché, Yilun Du, Yaroslav Ganin, Arthur Mensch, Will Grathwohl, Nikolay Savinov, Sander Dieleman, Laurent Sifre, and Rémi Leblond. Self-conditioned embedding diffusion for text generation. abs/2211.04236, 2022. 3

Ashish Vaswani, Noam Shazeer, Niki Parmar, Jakob Uszkoreit, Llion Jones, Aidan N. Gomez, Lukasz Kaiser, and Illia Polosukhin. Attention is all you need. 2017. 1

Guanghan Wang, Yair Schiff, Subham Sekhar Sahoo, and Volodymyr Kuleshov. Remasking discrete diffusion models with inference-time scaling. abs/2503.00307, 2025. 3

Zhisheng Xiao, Karsten Kreis, and Arash Vahdat. Tackling the generative learning trilemma with denoising diffusion gans. 2022. 4

Jiacheng Ye, Shansan Gong, Liheng Chen, Lin Zheng, Jiahui Gao, Han Shi, Chuan Wu, Xin Jiang, Zhenguo Li, Wei Bi, and Lingpeng Kong. Diffusion of thought: Chain-of-thought reasoning in diffusion language models. 2024. 3

Jiacheng Ye, Zhihui Xie, Lin Zheng, Jiahui Gao, Zirui Wu, Xin Jiang, Zhenguo Li, and Lingpeng Kong. Dream 7b, 2025. URL https://hkunlp.github.io/blog/2025/dream. 2, 3

Qiying Yu, Zheng Zhang, Ruofei Zhu, Yufeng Yuan, Xiaochen Zuo, Yu Yue, Tiantian Fan, Gaohong Liu, Lingjun Liu, Xin Liu, et al. Dapo: An open-source llm reinforcement learning system at scale. 2025. 3

Weihao Zeng, Yuzhen Huang, Qian Liu, Wei Liu, Keqing He, Zejun Ma, and Junxian He. Simplerl-zoo: Investigating and taming zero reinforcement learning for open base models in the wild. 2025. 3

Siyan Zhao, Devaansh Gupta, Qinqing Zheng, and Aditya Grover. d1: Scaling reasoning in diffusion large language models via reinforcement learning. 2504.12216, 2025. 3, 8

Rui-Jie Zhu, Tianhao Peng, Tianhao Cheng, Xingwei Qu, Jinfa Huang, Dawei Zhu, Hao Wang, Kaiwen Xue, Xuanliang Zhang, Yong Shan, Tianle Cai, Taylor Kergan, Assel Kembay, Andrew Smith, Chenghua Lin, Binh Nguyen, Yuqi Pan, Yuhong Chou, Zefan Cai, Zhenhe Wu, Yongchi Zhao, Tianyu Liu, Jian Yang, Wangchunshu Zhou, Chujie Zheng, Chongxuan Li, Yuyin Zhou, Zhoujun Li, Zhaoxiang Zhang, Jiaheng Liu, Ge Zhang, Wenhao Huang, and Jason Eshraghian. A survey on latent reasoning, 2025. 8
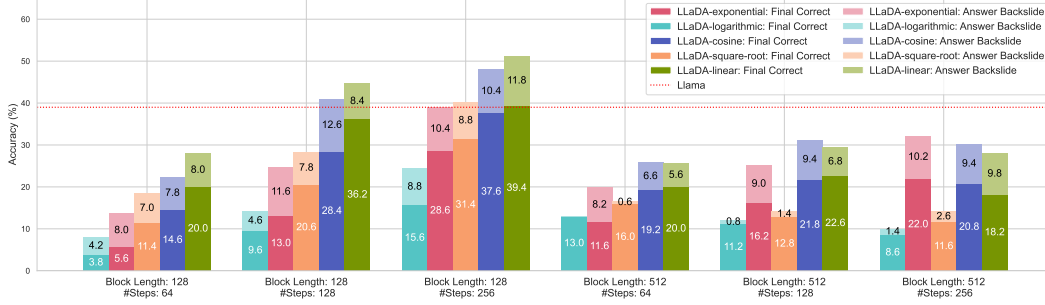
A   TECHNICAL APPENDICES AND SUPPLEMENTARY MATERIAL

Figure 5: Comparison of different re-masking strategies introduced by MaskGIT.

A.1   TRAINING-INFERENCE DISCREPANCY

In Section 3.4, we introduce the two remasking strategies from LLaDA, random remasking and low-confidence remasking (LCR). As the tokens are also randomly masked in pre-training, and LCR is usually used as the de-facto standard for inference (Nie et al., 2025), analyzing the difference between random remasking and low-confidence remasking provides us a closer look at the training-inference divide. Table 3 shows concrete examples to demonstrate the difference between random masking and LCR.

We observe that LCR consistently produces more coherent and complete masked intermediate completions compared to random remasking at the same masking ratio. At high masking ratios (e.g., 0.75 at Step 16), random remasking often fails to preserve the problem structure, leading to fragmented or nonsensical outputs, whereas LCR retains recognizable mathematical expressions and approaches the ground truth earlier. As the masking ratio decreases (Steps 32 and 48), the gap narrows, while LCR still maintains a higher degree of structural integrity.

A.2   REMASKING SCHEDULING FUNCTION

The remasking scheduling function ϕ introduced in Section 3.4 defines how many tokens should be masked at every timestep, which can also influence the generation performance. Though the choices of ϕ is not discussed in the LLaDA paper, multiple design choices of the ϕ are studied in MaskGIT (Chang et al., 2022) for image generation tasks. We list the definitions of these functions as following

$$\phi\left(t,T\right) = \begin{cases} \dfrac{e - e^{\frac{t}{T}}}{e - 1}, & \text{Exponential} \\[2mm] 1 - \left(\dfrac{t}{T}\right)^{3}, & \text{Cubic} \\[2mm] 1 - \left(\dfrac{t}{T}\right)^{2}, & \text{Square} \\[2mm] \dfrac{1 + \cos\left(\pi\,\frac{t}{T}\right)}{2}, & \text{Cosine} \\[2mm] 1 - \dfrac{t}{T}, & \text{Linear} \\[2mm] 1 - \sqrt{\dfrac{t}{T}}, & \text{Square Root} \\[2mm] 1 - \dfrac{\ln\left(1 + \frac{t}{T}\right)}{\ln(2)}, & \text{Logarithmic} \end{cases} . \tag{11}$$

Out of these functions, LLaDA uses the linear strategy that the same amount of tokens are *not* remasked at each step. We conduct evaluation with the representative ones: exponential (exp),
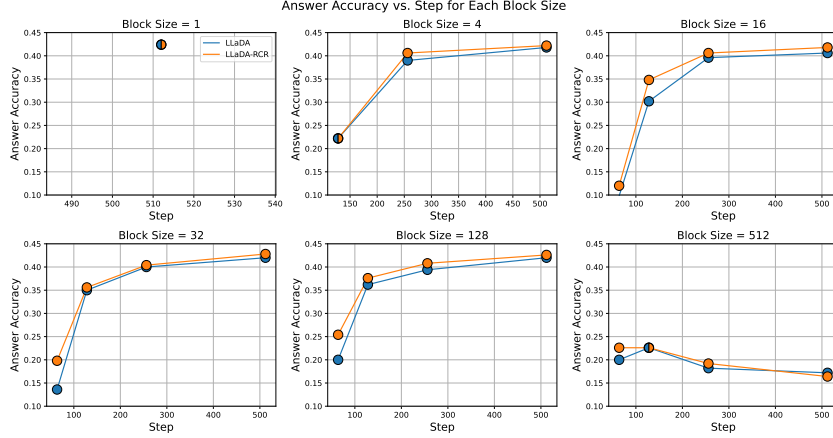
Figure 6: Interpolation of block sizes and number of time steps to investigate the effect of these two factors on the inference performance. Generation length is fixed to 512.

logarithmic (log), cosine, square root, and linear, on the MATH-500 task. Results in Fig. 5 show that the linear strategy works the best, which is not consistent with MaskGIT on image synthesis, where the concave functions like cosine that follows a less-to-more generation procedure works better.

A.3 BLOCK SIZE IN SEMI-AR

As discussed in Section 4.1, a key factor that affects the performance of MDLMs is the block size. When block size $B = L$ where L is the generation length, the model denoises all the tokens simultaneously which we refer to as *pure-Diff*. And we refer to $B < L$ as *semi-AR* where the sequence is divided into several blocks and generated from left to right. Within each block, tokens are denoised in parallel.

To better understand the interplay between block size and the number of denoising steps, we conduct experiments with LLaDA-Instruct on the MATH-500 benchmark, varying $B \in 1, 4, 16, 32, 128, 512$ and the number of steps $T \in 32, 64, 128, 256, 512$. The results in Fig. 6 reveal several trends: (1) Small block sizes (e.g., $B = 4$) show slower initial gains but benefit more from increasing T, indicating that finer-grained autoregression allows iterative refinement over more steps; (2) Medium block sizes (e.g., $B = 16, 32, 128$) achieve the highest accuracy at moderate T, suggesting a favorable balance between parallelism and left-to-right dependency modeling; (3) pure-Diff (i.e., $B = 512$) consistently underperforms, and accuracy even drops at higher T, implying that excessive parallel denoising hinders the model's ability to progressively refine solutions on math tasks. However, as discussed earlier following Table 2, pure-Diff is more flexible in dealing with tasks that require answers with varied length, e.g., Countdown. Therefore, improving the performance of pure-Diff is as well crucial to the wider application of masked diffusion language models.

Table 3: Compare random remasking and confidence-based remasking. We show the model completions at selected steps (16, 32, 48) given a prompt, with the remasked tokens ([M]) by random remasking and LCR with a mask ratio corresponding to the respective step.

Prompt	Define $p = \sum_{k=1}^\infty \frac{1}{k^2}$ and $q = \sum_{k=1}^\infty \frac{1}{k^3}$. Find a way to write $\sum_{j=1}^\infty \sum_{k=1}^\infty \frac{1}{(jk)^3}$ in terms of p and q.
Ground Truth	\boxed{p - q}
Step 16: Completion	We can write\n \[\sum_{j = 1}^\infty \sum_k = 1^\infty \frac1(j + k)^3 = \sum_1 = 1^ \infty \frac1k^^ = \boxed{pboxed{p - q}.\]
Masking Ratio 0.75	
Random	[M][M][M][M]\[\[M][M][M][M] [M][M][M][M]sum[M][M] [M][M]1[M]infty \[M][M][M][M][M][M][M][M][M][M] = \[M][M][M][M][M]1[M][M][M][M]{[M]}{k^[M][M][M][M] [M][M][M][M][M][M][M][M]
LCR	We can write\n \[\[M]_{[M] = 1[M]infty[M][M][M][M][M] [M][M][M][M][M][M][M][M][M][M][M][M][M][M][M][M] [M][M][M][M][M][M][M][M][M][M][M][M][M][M][M] [M][M][M][M][M][M][M][M] - q}.\]
Step 32: Completion	We can write\n\[\sum_{j = 1}^\infty \sum_{k = 1}^\infty \frac{1}{(j + k)^3} = \sum_{j = 1}^\infty \frac{1}{k^^} = \boxed \boxed{p - q}.\]
Masking Ratio 0.5	
Random	[M] can write[M]\[\[M]_{j[M] 1[M]infty \sum[M][M][M] [M]}^\[M] \[M][M]1[M][M] +[M][M]3[M] =[M][M]_{j =[M]1}^\infty\frac[M]1}{[M][M][M][M] =[M][M]\[M][M][M][M]}.[M][M][M]
LCR	We can write\n\[\sum_{j = 1}^\infty \sum_{k = 1}^\infty \frac{1[M][M][M][M][M][M][M][M][M][M][M][M][M][M] [M][M][M][M][M][M][M][M][M][M][M][M][M][M][M] [M][M] - q}.\]
Step 48: Completion	We can write \n\[\sum_{j = 1}^\infty \sum_{k = 1}^\infty \frac{1}{(j + k)^3} = \sum_{j = 1}^\infty \frac{1}{j^3} = \boxed{p}{{p - q}.\]
Masking Ratio 0.25	
Random	We[M] write [M]sum[M]j[M] 1}^\infty[M]sum_{k =[M][M][M]infty \[M]{[M]}{(j + k[M]3} =[M]sum_{[M] = 1}^\infty \[M]1{j^3[M] =[M][M]{p}{{p - q}.\]
LCR	We can write\n\[\sum_{j = 1}^\infty \sum_{k = 1}^\infty \frac{1}{(j + k)^3} = \sum_{[M] = 1}^\infty[M][M][M][M][M][M][M][M][M][M][M][M][M][M][M] - q}.\]
Step 64: Final Completion	We can write\n\[\sum_{j = 1}^\infty \sum_{k = 1}^\infty \frac{1}{(j + k)^3} = \sum_{j = 1}^\infty \frac{1}{j^3} = \boxed{2p - q}.\]